Neutron scattering study of magnetic ordering in the double-layer antiferromagnet $K_3Mn_2F_7$

C. M. J. van Uijen
Fysisch Laboratorium, Rijksuniversiteit, P.O. Box 80.000, 3508 TA Utrecht, The Netherlands

E. Frikkee
Netherlands Energy Research Foundation ECN, 1755 ZG Petten (N.H.), The Netherlands

H. W. de Wijn
Fysisch Laboratorium, Rijksuniversiteit, P.O. Box 80.000, 3508 TA Utrecht, The Netherlands

(Received 10 July 1978)

Elastic and quasielastic scattering of neutrons from the double-layer Heisenberg antiferromagnet with weak anisotropy $K_3Mn_2F_7$ has been employed to study the magnetic structure, the variation with temperature of the sublattice magnetization, the generalized susceptibility, and the spin-spin correlation length. At $T_N = 58.3 \pm 0.2$ K $K_3Mn_2F_7$ exhibits a second-order phase transition to antiferromagnetic order with the spins aligned along the tetragonal axis. In the low-temperature region, the sublattice magnetization excellently follows a previous renormalized spin-wave result up to $\sim T_N/2$. Near T_N, the critical exponent for the order parameter is $\beta = 0.154 \pm 0.006$. As is the case in single-layer structures, neutron scattering from spin-spin correlations above T_N occurs along ridges in reciprocal space, with the noticeable difference that in the double-layer structure these ridges are modulated in intensity due to interference of the paired layers separated by $\delta = 4.18 \pm 0.07$ Å, while at 4 K $a = 4.181 \pm 0.003$ Å and $c = 21.55 \pm 0.02$ Å. From the development of the ridge profile, the critical exponents for the generalized susceptibility $\chi(\vec{q})$ and inverse correlation length are found to be $\gamma = 1.9 \pm 0.3$ and $\nu = 1.1 \pm 0.2$, and from these, with $\nu(2-\eta) = \gamma$, $\eta = 0.20 \pm 0.05$ for the deviation from the Ornstein-Zernike $\chi(\vec{q})$. The critical exponents are essentially equal to those in comparable single-layer systems, such as K_2MnF_4 and Rb_2MnF_4, while they do not differ substantially from the exact two-dimensional Ising results. In addition, in $K_3Mn_2F_7$ spin-spin correlation near T_N extends over essentially the same length as in single layers. The general conclusion is that the phase transition in Heisenberg double-layer systems is of strictly two-dimensional nature. At $\sim 1.5T_N$, however, evidence is found for a more rapid decrease of the correlation length than in single layers, suggesting transition to three-dimensional behavior.

I. INTRODUCTION

Recently, the magnetic properties of the antiferromagnet $K_3Mn_2F_7$ have been examined in some detail. The interest in this system is connected with its particular magnetic structure, the quadratic double layer with nearest-neighbor Heisenberg exchange interaction and weak anisotropy, which may be viewed as a first step from the well-studied two-dimensional (2-D) system K_2MnF_4 towards the three-dimensional (3-D) perovskite $KMnF_3$. For $K_3Mn_2F_7$, all magnetic properties studied up till now, including the susceptibility in the ordered and paramagnetic regime,[1,2] the sublattice magnetization,[3] and two-magnon Raman scattering,[4] seem to indicate that the magnetic behavior of the double layer is closer to 2-D than 3-D, at least well below T_N. In the critical regime, however, no conclusions have been arrived at as yet. A principal objective of the present investigation therefore is to study the critical behavior of $K_3Mn_2F_7$ by elastic-neutron-diffraction techniques, and to present a comparison with the single-layer 2-D systems on one hand and the "infinite-layer" 3-D systems on the other hand.

The principal examples of the single-layer systems, the almost genuine 2-D Heisenberg systems with

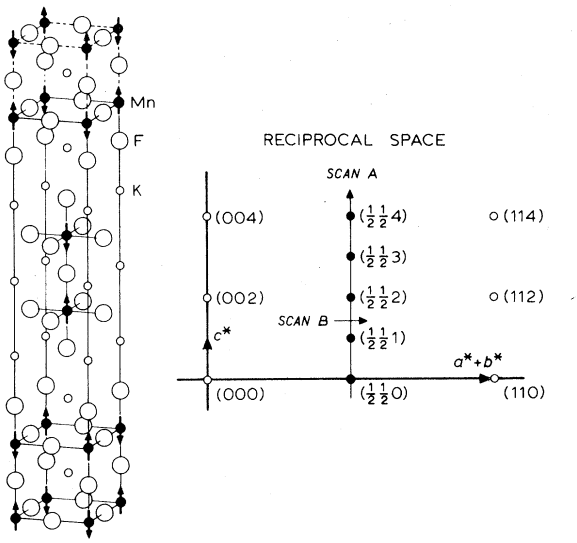

FIG. 1. Crystallographic unit cell of $K_3Mn_2F_7$. To indicate more clearly the double-layer structure, the cell has been extended along the tetragonal axis. The lattice parameters are $a = 4.181 \pm 0.003$ Å and $c = 21.55 \pm 0.02$ Å at 4.2 K. Neutron scattering momentum transfer is in the $(1\bar{1}0)$ plane. In reciprocal space, with the indexing $(h\ k\ l)$ based on the crystallographic unit cell, open circles denote nuclear reflections and closed circles magnetic Bragg peaks. Nuclear reflections with l odd are symmetry forbidden. Scans of types A and B are along and across the ridge of magnetic scattering, respectively.

small anisotropy K_2MnF_4, K_2NiF_4, and Rb_2MnF_4, which we will use as a reference below, have been examined in great detail by neutron diffraction[5–9] as well as a variety of other techniques.[10,11] The general conclusions are as follows. It is well established that 2-D renormalized spin-wave theory properly accounts for the thermodynamic properties of these 2-D systems in the temperature region below, say, $\frac{1}{2}T_N$.[12] The 2-D character of the spin waves is confirmed by inelastic neutron work,[7] which proved the magnon dispersion to be negligible along the c axis. The critical behavior has also been the subject of many studies. Since in a 2-D array of spins with Heisenberg interaction only long-range order cannot exist at finite temperatures,[13] the occurrence of a phase transition in K_2MnF_4 and its isomorphs is apparently governed by the small anisotropy in the system.[14] In addition, although the system, when it orders, does so in three dimensions because of residual magnetic interactions in the third dimension, the transition itself is 2-D in character.[6] This may be inferred from the critical exponent β ($\beta = 0.15 \pm 0.01$ in K_2MnF_4)[7], which is found to be close to that of the exactly solvable 2-D Ising model ($\beta = \frac{1}{8}$),[15] rather than that belonging to 3-D models ($\beta \approx \frac{1}{3}$).

As is the case for the single-layer 2-D systems, the low magnetic dimensionality of $K_3Mn_2F_7$ originates from its crystal structure (Fig. 1). The double-layer structure $K_3Mn_2F_7$ may be constructed from K_2MnF_4 by substituting unit cells of $KMnF_3$ in place of the MnF_2 squares in K_2MnF_4. The argument of cancellation of magnetic interactions between adjacent layers in K_2MnF_4 is equally valid for the double-layer structure, i.e., there is no net magnetic interaction between adjacent double layers, at least not for the $k = 0$ magnon mode. Further, the interaction between next-nearest double layers is many orders of magnitude weaker than the intralayer nearest-neighbor exchange because of the large distance involving many intermediate ions, so that indeed $K_3Mn_2F_7$ closely represents an isolated double-layer system.

Elastic-neutron-scattering work on another representative of double-layer systems, $Rb_3Mn_2Cl_7$, has been reported by Gurewitz *et al.*[16] In their experiments the emphasis was on the structure, including the magnetic registry of the next-nearest-neighbor double layers, which turned out to be ferromagnetic or antiferromagnetic dependent on the sample preparation. In particular, they unambiguously proved the double-layer character by observing the rods of scattering in reciprocal space, in themselves typical for a 2-D system, to be modulated with a periodicity, directly related to the distance between the paired layers.

Recent susceptibility measurements[1,2] on $K_3Mn_2F_7$ and isomorphs reveal that the broad maximum above T_N (~ 58 K in $K_3Mn_2F_7$), reflecting the amount of short-range correlations, is substantially reduced in comparison with single-layer systems, and thus confirm the prediction based on the high-temperature expansion[17] that the susceptibility in this region is between 2-D and 3-D. In the ordered regime, however, the sublattice magnetization, measured up to 40 K with NMR techniques and analyzed in terms of spin-wave theory,[3] exhibits a 2-D temperature dependence, apart from a scaling factor originating from the different coordination of the magnetic sites. This is because at low temperatures only those spin waves are excited for which the spins in the paired layers precess in phase with one another ($k_z = 0$). The other magnon branch, which corresponds to out-of-phase precession of the paired layers, i.e., involving excitations of the spin system in the third dimension, requires a substantially larger energy ($\geq 4|J|S$), and is not yet appreciably populated. The zero-point spin reduction, however, to which all possible excitations in the Brillouin zone contribute without being weighed by a Bose factor, is computed to be 0.124,[3]

intermediate between 2-D ($\Delta S = 0.17$ for K_2MnF_4) and 3-D ($\Delta S = 0.078$ for $KMnF_3$).

As already said, the main purpose of the present investigation is to study the nature of the phase transition in the antiferromagnetic double layer $K_3Mn_2F_7$ in comparison with single-layer and 3-D systems. To this end, we employ the techniques of elastic as well as quasielastic critical magnetic scattering of neutrons to measure the variation with temperature of the sublattice magnetization M and the wavelength-dependent susceptibility $\chi(\vec{Q})$. In particular, we will focus on the asymptotic behavior near T_N of M, $\chi(\vec{Q})$, and the inverse correlation length, in order to determine their critical exponents β, γ, and ν, respectively. Additionally, the experiments yield the magnetic structure in the ordered phase.

II. NEUTRON SCATTERING

A. Experimental

In Fig.1, the scattering configurations used are illustrated in reciprocal space. In all configurations the momentum transfer is in the $(1\bar{1}0)$ plane. The nuclear reflections are indicated by open circles, while the magnetic Bragg scattering in the ordered phase occurs at the reciprocal superlattice positions marked by closed circles. However, for a system of spins ordered in two dimensions elastic Bragg scattering of neutrons is expected to occur along lines in reciprocal space ("ridges" of scattering), rather than points (peaks), as was first pointed out by Birgeneau *et al.*[6] in connection with neutron scattering in K_2NiF_4. In addition, these ridges contain the critical part of the scattering due to fluctuations in these 2-D arrays of spins. The $[1\bar{1}0]$ axis of the sample was oriented at right angles to the plane of scattering in order to allow scans along (scan A in Fig.1) as well as perpendicular (scan B) to the ridge $(\frac{1}{2}\frac{1}{2}l)$. With respect to the latter scans the choice of this geometry should be viewed as a compromise between the $\vec{Q}$ resolution of the spectrometer and the requirements of the quasielastic approximation (see Sec. III C), which dictates the final wave vector to be parallel to the ridge.

All data presented in this paper were taken on one of the two-axis spectrometers at the HFR reactor in Petten, using the (002) reflection of a Zn monochromator crystal to obtain a neutron beam with a wavelength of 1.473 Å. To enhance the resolution of the spectrometer both horizontal and vertical 30 minutes collimation was employed before and after the scattering. The crystal was grown with the horizontal zone melting technique, and had a mosaic spread of 0.3 degrees. In growing single crystals of $K_3Mn_2F_7$ with the size required in the neutron scattering experiments (50 mm^3), contaminations by small amounts of $KMnF_3$ and K_2MnF_4 appeared to be unavoidable. The sample used contained 1.5-vol% $KMnF_3$ and 0.9-vol% K_2MnF_4. The crystal was mounted in the cryostat on an aluminum crystal holder. Control of the temperature was accomplished by a servostabilized stream of boiled-off He gas to within 0.03 K over longer periods of time. Temperature measurements were done with a calibrated Ge resistor, and had an estimated inaccuracy of 1%. In the data analysis in the critical region, temperatures were taken relative to the transition point T_N, and these differences in temperature can be determined to better accuracy, 0.05 K or 2%, whichever is greater.

B. Cross section

In this section, we recapitulate the general features of magnetic scattering of unpolarized neutrons, in so far as relevant to the analysis of our experiments (Sec.III). For a more detailed review one is referred to the article by Marshall and Lowde.[18] Defining the scattering vector and the energy transfer of the neutrons by $\vec{Q} = \vec{k}_i - \vec{k}_f$ and $\hbar\omega = (\hbar^2/2m_n)(k_i^2 - k_f^2)$, with $\vec{k}_i$ and $\vec{k}_f$ the initial and final wave vector, respectively, and m_n the neutron mass, the double-differential cross section for magnetic scattering reads

$$\frac{d^2\sigma}{d\Omega\, dE} = A(\vec{k}_i, \vec{k}_f) \sum_{\alpha\beta} (\delta_{\alpha\beta} - \hat{Q}_\alpha \hat{Q}_\beta) S^{\alpha\beta}(\vec{Q}, \omega) \quad . \tag{1}$$

Here, $\alpha, \beta = x,y,z$, while $A(\vec{k}_i, \vec{k}_f)$ is proportional to $(k_f/k_i)|f(\vec{Q})|^2$, with $f(\vec{Q})$ the magnetic form factor, for which numerical results are available in the literature.[19] The quantity $S^{\alpha\beta}(\vec{Q}, \omega)$ represents the scattering function

$$S^{\alpha\beta}(\vec{Q}, \omega) = \frac{1}{2\pi} \sum_{\vec{r}} \int_{-\infty}^{\infty} dt\, e^{i(\vec{Q}\cdot\vec{r} - \omega t)} \times \langle S^\alpha(\vec{0}, 0) S^\beta(\vec{r}, t) \rangle \quad , \tag{2}$$

i.e., the space-time Fourier transform of the two-spin correlation function. For the systems of interest here, having Heisenberg exchange coupling and uniaxial anisotropy, $S^{\alpha\beta}(\vec{Q}, \omega)$ is diagonal.

The scattered intensity is usually split into an elastic Bragg part, proportional to the square of the sublattice magnetization, and a diffuse part arising from fluctuations of the spins about their thermal average. For an antiferromagnet with the spins along an easy z axis (not necessarily coinciding with the tetragonal axis) the former may be written

$$\left(\frac{d\sigma}{d\Omega}\right)_{\text{Bragg}} \propto \langle S^z \rangle^2 \exp[-2W(\vec{Q})] |F_M(\vec{Q})|^2 \times (1 - \hat{Q}_z^2) \delta(\vec{Q} - \vec{\tau}) \quad . \tag{3}$$

Here, $W(\vec{Q})$ is the Debye-Waller factor, $\vec{\tau}$ is a reciprocal-lattice vector, and

$$F_M(\vec{Q}) = f(\vec{Q}) \sum_{\vec{d}} \sigma_{\vec{d}} e^{i\vec{Q}\cdot\vec{d}} \tag{4}$$

is the magnetic structure factor, in which the summation runs over all spins in the magnetic unit cell at position $\vec{d}$, and $\sigma_{\vec{d}} = \pm 1$ for the up or down sublattice.

The remaining part of the scattering, arising from fluctuations in the magnetization, is proportional to the space-time Fourier transform of the correlation function $\langle \delta S^\alpha(\vec{0},0)\delta S^\beta(\vec{r},t)\rangle$, where

$$\delta S^\beta(\vec{r},t) = S^\beta(\vec{r},t) - \langle S^\beta(\vec{r},t)\rangle$$

represents the fluctuations of the order parameter about its thermal average. For critical fluctuations under normal conditions the major contributions to the scattering come from the region $\hbar\omega << k_B T$. If further all neutrons emerging at a given scattering angle are collected irrespective of their energy and the scattering geometry is such that the spread in k_f due to inelasticity is small relative to the inverse correlation length, i.e., adopting the quasielastic approximation, the diffuse part of the cross section turns out to be

$$\left(\frac{d\sigma}{d\Omega}\right)_{\text{diff}} \propto \sum_\alpha (1-\hat{Q}_\alpha^2) \times \int_{-\infty}^{\infty} d\omega \; [S^{\alpha\alpha}(\vec{Q},\omega) - S^{\alpha\alpha}_{\text{Bragg}}(\vec{Q},\omega)]$$

$$= \frac{k_B T}{g^2 \mu_B^2} \sum_\alpha (1-\hat{Q}_\alpha^2)\chi^{\alpha\alpha}(\vec{Q}) \; . \tag{5}$$

Thus, the diffuse scattering cross section is a direct measure of the generalized susceptibility $\chi^{\alpha\beta}(\vec{Q})$. Discussion of the validity of the quasielastic approximation in our experimental arrangement is deferred to Sec. III C.

III. EXPERIMENTAL RESULTS

In this section we successively discuss in detail the magnetic Bragg scattering and the diffuse scattering, as well as the physical quantities that can be extracted from them, i.e., the magnetic structure, the variation of the sublattice magnetization with temperature, and the wavelength-dependent susceptibility, including the critical exponents.

A. Magnetic structure

It has been established that the single-layer two-dimensional (2-D) systems, such as K_2MnF_4 and K_2NiF_4, once they order by going through T_N, actually gain long-range order in three dimensions (3-D LRO).[6] This is not in contradiction with the essentially 2-D magnetic character of these systems, but is simply due to the fact that the small interlayer exchange interaction, when summed over large areas of the layers, still constitutes a macroscopic energy. According to the present study, the double layer $K_3Mn_2F_7$ appears to behave similar to the single-layer structures: Below T_N evidence for near to complete 3-D LRO is found by the occurrence of magnetic Bragg scattering at points in reciprocal space rather than "rods" extending in a direction perpendicular to the layers of ordered spins. If we adopt indexing in reciprocal space with reference to the crystallographic cell, as will be done throughout this paper, the Bragg peaks below T_N are observed at the superlattice positions (hkl) with h and k half integer, and in our experimental arrangement $h = k$. In our experiments we observed magnetic Bragg peaks at integer l, rather than superlattice half integer, so that the stacking along the c axis is concluded to be ferromagnetic. In this context it is noteworthy that ferromagnetic stacking of next-nearest-neighbor (nnn) double layers has also been reported in $Rb_3Mn_2Cl_7$ crystals grown, as our crystals, from the melt.[16]

Two other points of interest regarding the structure, which both can be inferred from the relative intensities of the magnetic Bragg reflections, are the orientation of the spins in the ordered state and the distance δ between the paired layers. In such an analysis it is important to distinguish between reflections with odd and even index l, originating from domains in the crystal with the spin at the $\frac{1}{2}\frac{1}{2}\frac{1}{2}$ position parallel [(+) domain] and antiparallel [(−) domain] to the one at the origin, respectively. Since *a priori* the two types of domains may not be of equal occurrence, one has to extract the spin orientation and the paired-layer distance from the intensity ratios of Bragg peaks belonging to the same domains, i.e., $I(\frac{1}{2}\frac{1}{2}3)/I(\frac{1}{2}\frac{1}{2}1)$ for the (+) domains and $I(\frac{1}{2}\frac{1}{2}4)/I(\frac{1}{2}\frac{1}{2}2)$ for the (−) domains. In Table I we compare calculated relative intensities in the two domains with the experimental results at 4.2 K, with the Lorentz factor properly taken into account. Here, the distance δ between the paired layers is taken equal to the intralayer $Mn^{2+}-Mn^{2+}$ distance, which

TABLE I. Experimental intensity ratios of 3-D magnetic Bragg scattering in ordered $K_3Mn_2F_7$, as compared with calculated ratios in case $\delta = a$.

Ratio	Experiment	Calculated	
		∥ c axis	⊥ c axis
$I(\frac{1}{2}\frac{1}{2}4)/I(\frac{1}{2}\frac{1}{2}2)$	0.19 ± 0.02	0.19	0.53
$I(\frac{1}{2}\frac{1}{2}3)/I(\frac{1}{2}\frac{1}{2}1)$	1.39 ± 0.06	1.34	7.06

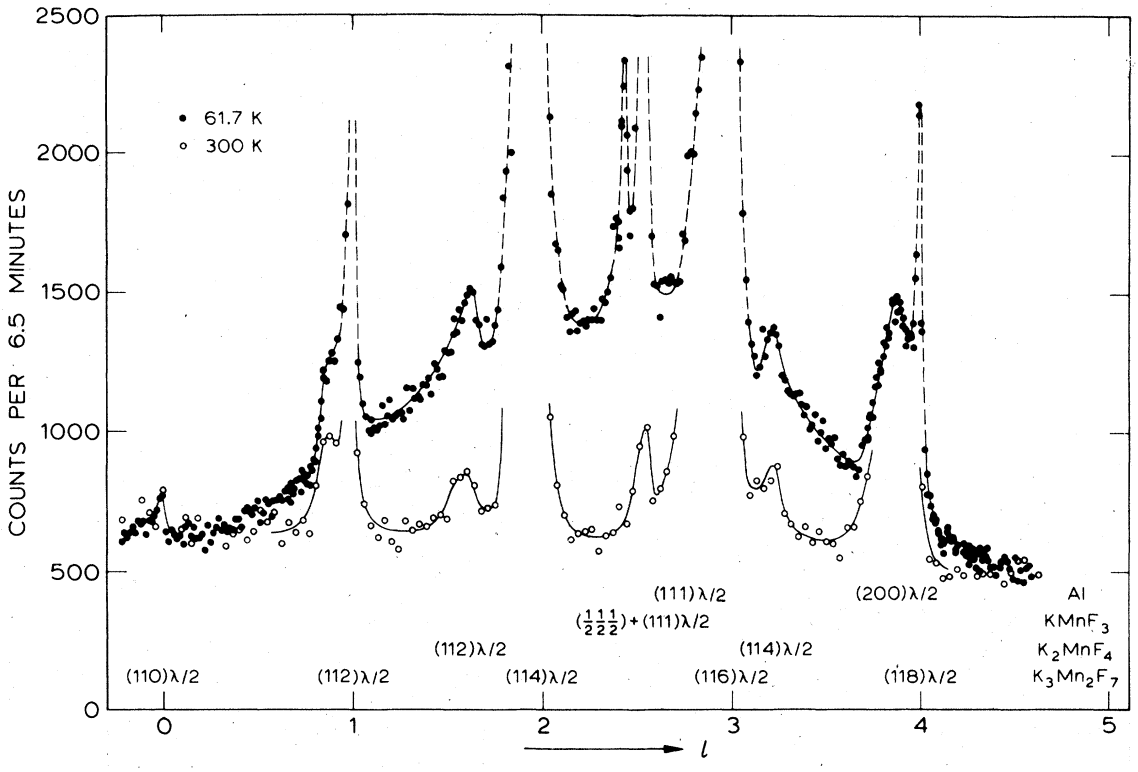

FIG. 2. Scan in reciprocal space along the top of the magnetic scattering ridge $(\frac{1}{2}\,\frac{1}{2}\,l)$ at 61.7 K (full circles; scan A in Fig.1). The magnetic double-layer structure results in vanishing ridge intensity at $l=0$ and $l\approx 5$ because of interference of the paired layers. To further demonstrate the magnetic origin of the ridge also a scan at 300 K is given (open circles). Peaks superimposed on the ridge originate from $\frac{1}{2}\lambda$ contamination of the primary neutron beam, giving rise to nuclear scattering in $K_3Mn_2F_7$, residual K_2MnF_4, and the Al sample holder. Also the $(\frac{1}{2}\,\frac{1}{2}\,\frac{1}{2})$ magnetic reflection in $KMnF_3$ ($T_N=88$ K), coinciding with the nuclear $(1\,1\,1)$ $\frac{1}{2}\lambda$, shows up weakly. Some smaller peaks are believed to originate from slight distortions.

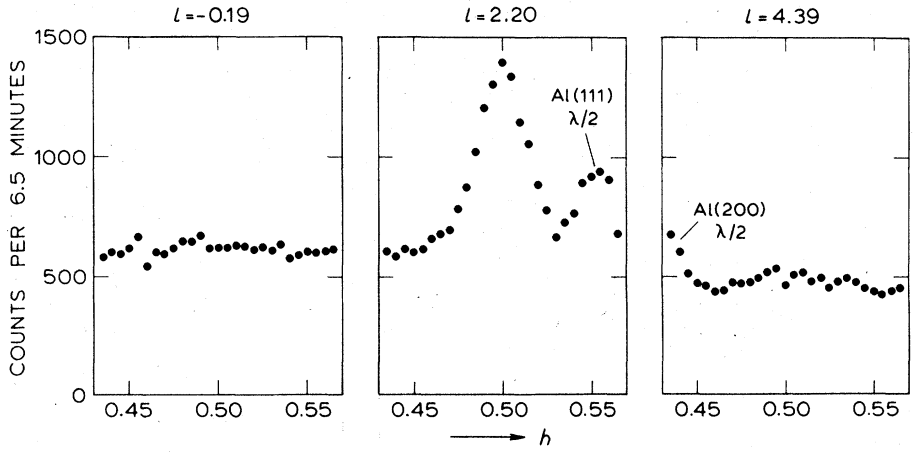

FIG. 3. Scans in reciprocal space transverse to the magnetic scattering ridge $(h\,k\,l)$ with $k=h$ at 61.7 K (scans of type B in Fig.1), demonstrating the absence of ridge intensity at the minima of the modulated ridge in Fig.2.

from nuclear Bragg scattering is found to be $a = 4.181 \pm 0.003$ Å at 4.2 K, while $c = 21.55 \pm 0.02$Å. Apparently, from the two most likely magnetic configurations in case of tetragonal symmetry, i.e., those with uniaxial or basal-plane anisotropy, the system favors the uniaxial anisotropy along the tetragonal axis, as is the case for $Rb_3Mn_2Cl_7$ and K_2MnF_4. In a more precise evaluation, in which δ is allowed to vary, the experimental intensity ratios are found to be consistent with the calculated ones for $\delta = 4.18 \pm 0.07$ Å, which within the experimental error equals the in-layer lattice constant.

As was pointed out by Birgeneau *et al.*,[6] critical scattering in a 2-D system as well as residual 2-D Bragg scattering are observed along rods in reciprocal space. However, in a double layer, because of antiferromagnetic coupling of the paired layers, these rods are modulated in intensity with a periodicity in l of c/δ, with a minimum at $l = 0$ imposed by symmetry. Therefore, by observing the ridge modulation, as was previously done for $Rb_3Mn_2Cl_7$, [16] one may directly confirm the double-layer character of the system. In Fig.2, a scan is shown along the ridge $(\frac{1}{2}\ \frac{1}{2}\ l)$ at 61.7 K, where it should be noted that the nuclear peaks superimposed on the ridge originate from $\frac{1}{2}\lambda$ contamination of the incident neutron beam. Additional scans transverse to the ridge at the positions $l = -0.19$, 2.20, and 4.39 (Fig.3) clearly demonstrate that in the scan along the rod at 61.7 K the ridge essentially disappears at the minima and the remaining intensity is background scattering. From the periodicity of the modulation, and taking into account the form factor [cf. Eq. (4)] and the variation of the background along the rod, we deduce $\delta = 4.4 \pm 0.4$ Å for the interlayer distance in agreement with δ from the relative Bragg intensities, but with a larger error.

B. Sublattice magnetization

As expressed by Eq. (3), the variation of the sublattice magnetization with temperature can be deduced from the intensity of magnetic Bragg peaks, where in the temperature region studied the effects of the Debye-Waller factor can safely be ignored. The measured intensities were corrected for the nuclear scattering of $\frac{1}{2}\lambda$ neutrons, which coincides with the magnetic Bragg scattering. This correction was set equal to the scattering remaining at temperatures substantially above T_N, where both the ridge and the magnetic Bragg peaks have vanished. Secondly, the ridge intensity at the reciprocal lattice points, which is of the order of 1% relative to the Bragg intensity at zero temperature, was determined by combining the results of scans of type A and B (see Fig.1) at various temperatures, and was subtracted off. Finally, the constant background was taken out. The reflection with the largest intensity and smallest statistical error within the practical range of the spectrometer is $(\frac{1}{2}\ \frac{1}{2}\ 2)$. To check on possible effects from extinction, the intensities of two other reflections, $(\frac{1}{2}\ \frac{1}{2}\ 3)$ and $(\frac{1}{2}\ \frac{1}{2}\ 4)$, were examined as well. The reduced sublattice magnetization $M(T)/M(0)$, as extracted from the $(\frac{1}{2}\ \frac{1}{2}\ 2)$ Bragg intensity, is given in Fig.4 from 4 K up to temperatures just above T_N.

In the low-temperature part of the ordered regime, the temperature dependence of $M(T)$ has previously been measured to high accuracy by NMR at the out-of-layer ^{19}F nucleus.[3] These data were found to excellently match a 2-D four-sublattice spin-wave theory appropriate to the Heisenberg double layer up to $\sim\frac{1}{2}T_N$. Temperature-dependent and independent corrections to the spin-wave energies due to magnon-magnon interactions were included up to first order. Least-squares fit of renormalized spin-wave theory to the NMR data yielded for the exchange constant $J/k_B = -7.59 \pm 0.03$ K, and for the zero-temperature energy gap $\epsilon_{k=0}/k_B = 5.99 \pm 0.06$ K. To compare the present data on the sublattice magnetization with spin-wave theory, the renormalized spin-wave calculation of the NMR study has been redone with the same spin-wave parameters, and inserted in Fig.4 as the solid line. Within the experimental inaccuracy of 2%, the neutron data agree well with the spin-wave result up to, say, 30 K, consistent with 28 K found from NMR. Confirming the NMR results, above this point there appears to occur a distinct departure of the sublattice magnetization from spin-wave theory, though at 30 K $\langle S^z \rangle$ has dropped by only 12% from the zero-temperature value. Upon increasing the temperature from 56 K, where 50% of the magnetization still remains, the magnetization disappears completely at 58.5 K, as is shown in the inset to Fig.4, with the system undergoing a second-order phase transition at 58.3 K. In the vicinity of the transition temperature T_N, the sublattice magnetization is usually described in terms of the power law

$$M(T)/M(0) = B[(T_N - T)/T_N]^{\beta} \ . \qquad (6)$$

In Fig. 5, the sublattice magnetization as deduced from the three magnetic Bragg reflections is presented in a log-log plot versus the reduced temperature $(T_N - T)/T_N$. Best fits of Eq. (6) to these data hold down to $(T_N - T)/T_N \approx 10^{-1}$, or $T \approx 52$ K, in contrast to the single-layer 2-D systems, where within the experimental errors the fit holds well into the spin-wave regime.[6] The three reflections, having quite different intensities, yield essentially the same critical parameters, $B = 0.83 \pm 0.03$ and $\beta = 0.154 \pm 0.006$, indicating that extinction effects are indeed negligible. In addition, the three plots give the same output value for the Néel temperature,

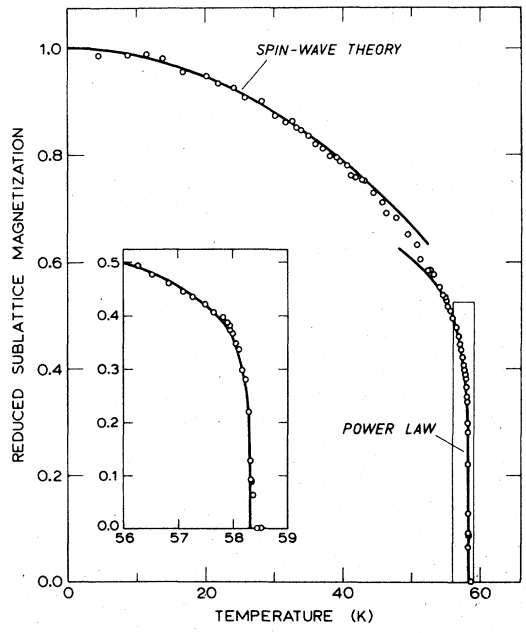

FIG. 4. Temperature dependence of the reduced sublattice magnetization in $K_3Mn_2F_7$ as measured from the intensity variation of the $(\frac{1}{2}\,\frac{1}{2}\,2)$ Bragg reflection. Below 30 K the data excellently match an earlier fit of renormalized spin-wave theory to NMR results (Ref.3). In the vicinity of the phase transition ($T_N = 58.3$ K) the sublattice magnetization has been fitted to a power law, with the fit extending down to 52 K.

$T_N = 58.28 \pm 0.05$ K. It should however be stressed that the inaccuracy quoted for T_N does not contain the uncertainty in the absolute calibration of the temperature sensor, a reasonable estimate of the actual error in T_N then being $T_N = 58.3 \pm 0.2$ K. The result obtained for B is significantly smaller than the exact result $B = 1.22$ for the 2-D Ising system and the experimentally found $B = 1.0$ in K_2NiF_4 and isomorphs.[6,7] A quantity that more intimately pertains to the critical behavior is the exponent β. For the double-layer structure $K_3Mn_2F_7$ β turns out to equal those found in Mn single-layer structures, 0.15 ± 0.01 in K_2MnF_4,[7] and 0.16 ± 0.01 in Rb_2MnF_4,[6] while approximating $\beta = 0.138 \pm 0.004$ in K_2NiF_4.[20] These critical exponents compare with the exact theoretical result for a 2-D Ising system, $\beta = \frac{1}{8}$, rather than the value for 3-D systems, $\beta \approx \frac{1}{3}$, obtained both theoretically[21] and experimentally.[22,23] This is illustrated in Fig.5, where we have plotted the theoretical prediction of Onsager for 2-D Ising systems,[15] and also have indicated the experimental results for K_2MnF_4,[7] and MnF_2.[22] The general conclusion therefore is that the antiferromagnetic-paramagnetic phase transition in $K_3Mn_2F_7$ is as strictly 2-D in nature, as in the single-layer systems. This conclusion is supported further by the observation that the diffuse scattering remains on ridges in reciprocal space when going through the transition point (cf. Sec.III C).

Upon closer inspection of the Bragg intensity versus temperature, it appears that the sublattice magnetization has not yet completely vanished at 58.28 K, and in fact the derivative dM/dT is not truly discontinuous at T_N, as it should be for a second-order phase transition. As was pointed out by Birgeneau *et al.*,[7] this effect possibly originates from a smearing of Néel temperatures due to some kind of inhomogeneities. A spread in T_N further causes the critical scattering (see Sec.III C) to peak at a temperature somewhat larger than the transition point obtained from a power-law fit to the sublattice magnetization. Adopting a Gaussian distribution of Néel temperatures with a mean $T_N = 58.28$ K, and following the procedure of Birgeneau *et al.*, we estimate from the temperature where the ridge intensity reaches its maximum, 58.45 ± 0.10 K, the relative standard deviation in the spread of T_N to be $\sigma' = 0.002$. Alternatively, σ' may be derived from the point where the magnetic Bragg peaks vanish, 58.35 ± 0.05 K, with the same result.

C. Critical scattering

It was already recalled in Sec.II that the temperature dependence of the wavelength-dependent susceptibility can be extracted from the diffuse part of the neutron-scattering cross section. However, as expressed by Eq. (5), this requires integration over the energy transfer by the neutron. Before discussing this in more detail, we first consider the development of the ridge with temperature at $l = 1.46$, the intensity of which is presented in Fig.6. This location on the ridge, although besides the maximum of the modulation, was chosen because of the absence of Bragg scattering, such as the (111) $\frac{1}{2}\lambda$ reflection of the Al sample holder, in transverse scans (cf. Fig.3 for $l = 2.20$). Upon lowering the temperature, the ridge intensity increases, apparently as a result of the divergence of the susceptibility at $T_N(1 + 1.5\sigma') = 58.45$ K (see Sec.III B). At the same time the width of the ridge reduces, indicating that the range of spin correlations within the double layer becomes larger when approaching T_N. In the ordered regime, three contributions may add to the total scattering. Just below T_N, the longitudinal component of the susceptibility $\chi^{\parallel}(=\chi^{zz})$, describing correlations of the fluctuations in the z component of the spins, drops rapidly with decreasing temperature, so that below ~ 50 K the scattering along the ridge is determined by the transverse spin fluctuations and the elastic magnetic scattering from 2-D ordered

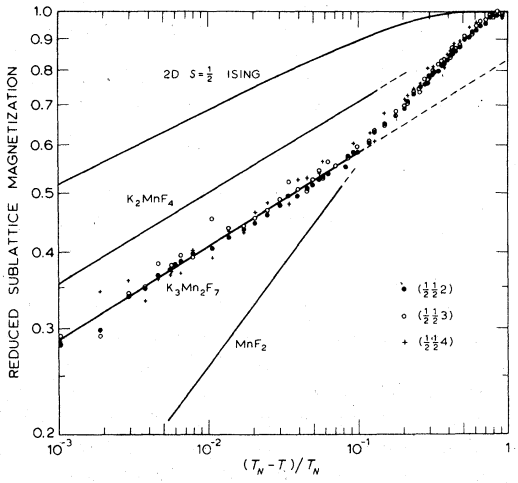

FIG. 5. Reduced sublattice magnetization in $K_3Mn_2F_7$, as deduced from various Bragg reflections, versus reduced temperature $(T_N-T)/T_N$ in a log-log plot, yielding the critical exponent $\beta=0.154\pm0.006$. For comparison, the experimentally found critical behavior of the single-layer structure K_2MnF_4 (Ref.7) and the 3-D structure MnF_2 (Ref.22) are also shown, as is the exact theoretical result by Onsager (Ref.15) for 2-D Ising systems ($\beta=\frac{1}{8}$).

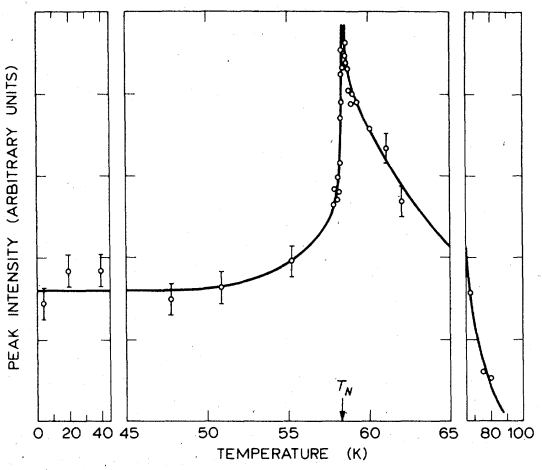

FIG. 6. Peak intensity of the $(\frac{1}{2}\frac{1}{2}l)$ ridge at $l=1.46$ vs temperature, with background scattering subtracted. At this position in reciprocal space the diffuse neutron cross section samples the generalized susceptibility as $0.86\chi^{\parallel}(\vec{Q})+1.14\chi^{\perp}(\vec{Q})$.

spins. Since the former contribution goes linearly with temperature, while the latter scales with the sublattice magnetization $M(T)$, the scattering in the temperature range from 50 down to, say, 20 K is dominated by the transverse spin fluctuations, i.e., by $\chi^{\perp}=\chi^{xx}+\chi^{yy}$. At the low-temperature end of the ordered regime, Bragg scattering from 2-D LRO dominates the ridge intensity. With respect to the width of the ridge, $\chi^{\perp}$ gives rise to a wider profile than $\chi^{\parallel}$, so that with the disappearance of $\chi^{\parallel}$ below T_N the measured width increases. Below ~50 K the width was found to remain constant down to about 20 K, at which point it starts to decrease to about twice the instrumental resolution at zero temperature. As shown in Fig.6, the combined effect of scattering from 2-D LRO and transverse spin fluctuations apparently results in a constant intensity of the ridge from ~50 K all the way down to 4 K.

Concerning the quantitative analysis of the diffuse scattering experiments, two details need some comment. First, as was pointed out by Birgeneau *et al.*,[8] in experiments on 2-D systems integration over the energy can be performed to very high accuracy by taking the final wave vector k_f of the neutrons parallel to the ridge ($\theta_f=0$). More precisely, fulfilling the so-called quasielastic approximation requires

$$(m_n\Gamma/\hbar k_i\kappa)\sin\theta_f \ll 1 \ , \tag{7}$$

where θ_f is the angle between k_f and the ridge, m_n is the neutron mass, $\hbar\Gamma$ is a characteristic energy width of the inelastic scattering, and κ is the inverse correlation length. However, due to the presence of $\frac{1}{2}\lambda$ nuclear scattering, it was not feasible to take the data at a geometry such that $\theta_f=0$, but instead all data were taken at $\sin\theta_f=0.24$. With $\hbar\Gamma\approx0.25$ meV, as inferred from the energy analysis of the critical scattering in K_2NiF_4,[8] and $\kappa=0.01$ Å^{-1} both at $(T-T_N)/T_N=0.08$ we estimate $m_n\Gamma/\hbar k_i\kappa\approx0.65$. We may therefore conclude that no appreciable errors will be introduced by adopting the quasielastic approximation.[8]

In making scans transverse to the ridge, one actually measures the convolution of the cross section and the resolution function. After separating the three contributions to the scattering at the ridge (see below), the final scattering profile for the longitudinal susceptibility was deconvoluted for the spectrometer resolution. This was performed by use of the parameterized form of the resolution function of two-axis spectrometers worked out by Cooper and Nathans.[24] The parameters involved, the horizontal and vertical collimations and the mosaic spread of the monochromator crystal (0.25°) and the sample (0.3°), were determined from the spectrometer geometry and measured resolution ellipses around the Bragg reflections $(\frac{1}{2}\frac{1}{2}1)$ and $(\frac{1}{2}\frac{1}{2}2)$. In the computer program employed, the $\vec{q}$ dependence of χ is assumed to have the analytical form known as the Fisher-Burford first approximant[25]

$$\chi(\vec{q})\propto 1/[1+(q/\kappa)^2]^{1-\eta/2} \ , \tag{8}$$

where $\vec{q}$ is taken with reference to the center of the ridge, and implicitly $\kappa_x=\kappa_y$, i.e., the correlations are isotropic within the double layer.

The unravelling of the three contributions in the ordered regime, with the ultimate aim to correct the longitudinal susceptibility above T_N for the perpendicular one, proceeds as follows. First, the scattering profile at 4.5 K measured transverse to the ridge was entirely ascribed to 2-D long-range order. The temperature dependence of the 2-D LRO scattering profile was assumed to scale with the magnetic Bragg peak intensities, i.e., the intensity will decrease with increasing temperature as the squared reduced sublattice magnetization, while half the width at half-maximum is kept at the value at 4.5 K (0.024 Å^{-1}). The scans across the ridge at temperatures up to 50 K were subsequently corrected for the 2-D LRO scattering, resulting in profiles whose amplitude appears to increase linearly with temperature, while half the width at half-maximum remains constant at ~ 0.03 Å^{-1}. Such a behavior is essentially what one would expect for the transverse susceptibility on the basis of the molecular-field approach, and thus gives confidence that the procedure is basically correct. A point of note is that the width found, after deconvolution for the instrumental width, compares well with the inverse perpendicular correlation length $\kappa^{\perp} = 0.02$ Å^{-1} obtained from spin-wave theory with the anisotropy parameter from recent AFMR measurements in $K_3Mn_2F_7$.[26] Above T_N, where the 2-D LRO component of the scattering has vanished, the perpendicular susceptibility decreases with increasing temperature, but is still of such a size that its contribution to the scattering must be subtracted off to obtain the scattering profile associated with the longitudinal susceptibility only. The amplitude and width of the profile of the perpendicular susceptibility above T_N are adopted to vary according to the critical exponents of the longitudinal component of the susceptibility in a self-consistent way, with the 2-D Ising values $\gamma = \frac{7}{4}$ and $\nu = 1$ as first approximations. However, in these power laws the temperature was referred to a shifted critical point $T_{\perp} \approx 46$ K, which is determined by the requirement that the half width equals the value below T_N(0.03 Å^{-1}) at the true critical temperature T_N. The temperature-dependent corrections thus obtained were subtracted off, and the remaining scattering profiles were finally deconvoluted for the spectrometer resolution in the way discussed above. It should be noted here that the data were not sufficiently accurate to allow a direct estimate for η from fitting the Fisher-Burford approximant to the ridge profile. Instead, in Eq. (8) $\eta = 0$ was taken, thus adopting the classical Ornstein-Zernike form for $\chi(\vec{q})$. Below 59 K, the correlations within the layers become of such long range that the resulting ridge is too narrow to be resolved with the resolution of the spectrometer across the ridge at $l = 1.46$ (half the width at half-maximum ~ 0.01 Å^{-1}).

The results of the analysis for the amplitude and width of the ridge, i.e., $\chi^{\parallel}(q=0)$ and $\kappa^{\parallel}$, are plotted double logarithmically in Figs.7 and 8, respectively. In the temperature region $0.015 < (T - T_N)/T_N < 0.2$, the susceptibility can be expressed in terms of the power law

$$\chi^{\parallel}(q=0) \propto [(T - T_N)/T_N]^{-\gamma} , \tag{9}$$

with $\gamma = 1.9 \pm 0.3$, while the inverse correlation length is found to vary according to

$$\kappa^{\parallel} = C[(T - T_N)/T_N]^{\nu} , \tag{10}$$

with $\nu = 1.1 \pm 0.2$ and $C = 0.13$ Å^{-1}. It should be noted at this point that the exponents found are quite sensitive to the correction made for the transverse susceptibility, and in fact the inaccuracy of $\chi^{\perp}$ is a major source of the errors in the critical exponents. However, the output values for γ and ν appear to be strongly correlated, so that their ratio is determined to a higher accuracy than would follow from the individual γ and ν. Detailed inspection of the analysis

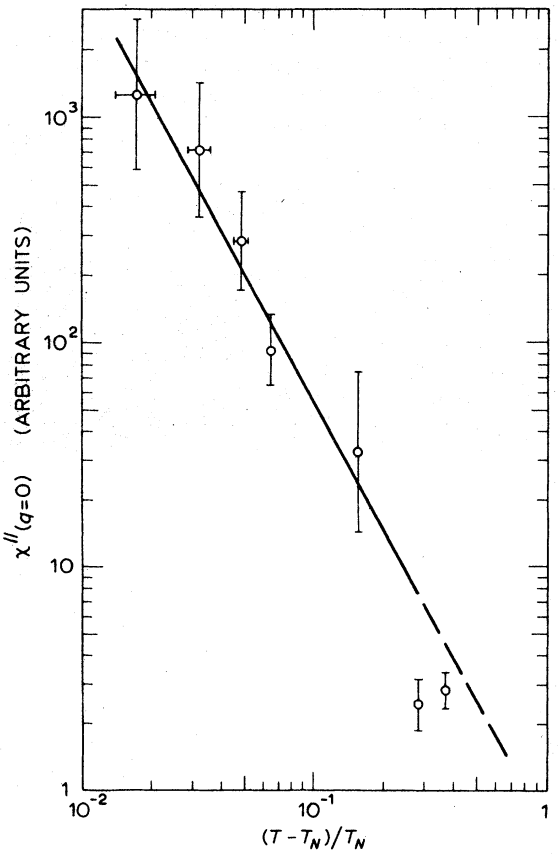

FIG. 7. Longitudinal susceptibility $\chi^{\parallel}(q=0)$, as derived from the height of the scattering ridge at $(\frac{1}{2}\ \frac{1}{2}\ 1.46)$ vs the reduced temperature in a log-log plot. Corrections have been made for the transverse susceptibility, while the data have been deconvoluted for the spectrometer resolution, as described in text.

yields $\gamma/\nu = 1.80 \pm 0.05$. From the exponent equality $\nu(2-\eta) = \gamma$ one then extracts $\eta = 0.20 \pm 0.05$ for the deviation from the classical Ornstein-Zernike form. The results are consistent with those for the exactly solvable 2-D Ising model ($\gamma = \frac{7}{4}$, $\nu = 1$, and $\eta = \frac{1}{4}$), as well as with the experimental findings for the single-layer structures[9] K_2NiF_4, K_2MnF_4, and $Rb_2Ni_{0.5}Mn_{0.5}F_4$ ($\gamma = 1.65 \pm 0.15$, $\nu = 0.95 \pm 0.10$, and $\eta \approx 0.2$), but differ from the exponents measured in the 3-D Heisenberg systems MnF_2 ($\gamma = 1.24 \pm 0.02$ and $\nu = 0.63 \pm 0.02$),[27] $RbMnF_3$ ($\gamma = 1.397 \pm 0.034$ and $\nu = 0.724 \pm 0.008$),[28] and $KMnF_3$ ($\gamma = 1.33 \pm 0.05$).[29] Thus, the present numerical results on the critical exponents in $K_3Mn_2F_7$ further support the conclusion arrived at in Sec. III B that the phase transition in double-layer antiferromagnets is essentially of 2-D nature.

IV. CONCLUDING REMARKS

Elastic as well as quasielastic neutron scattering data in $K_3Mn_2F_7$ were discussed in detail, and the main results can be summarized as follows.

(i) The system shows a second-order phase transition at 58.3 ± 0.2 K to antiferromagnetic long-range order within double layers, while the coupling of nnn double layers turns out to be ferromagnetic. The magnetic double-layer character was directly verified from the sinusoidal intensity modulation of the scattering along ridges in reciprocal space, where neutrons probe both 2-D spin correlations and 2-D LRO.[6] Further, from the intensity ratios of magnetic Bragg peaks the spins are concluded to be aligned parallel to the tetragonal axis. Elastic magnetic Bragg peaks with vanishing intensity at 58.0 ± 0.5 K have previously been reported for K_2MnF_4, and attributed to the occurrence of a Ca_2MnO_4-type magnetic structure, having antiferromagnetic nnn-layer coupling.[30] In view of the present results, however, it could very well be that some $K_3Mn_2F_7$ was present in the samples used in these experiments on K_2MnF_4.

(ii) The temperature variation of the sublattice magnetization, as derived from the intensity of three different magnetic Bragg scattering peaks, is found to be in excellent accord with previous NMR results.[3] In particular, it was confirmed that spin-wave theory appropriate to the double layer, even with renormalization to first order included, breaks down at $\sim \frac{1}{2} T_N$. As argued previously in connection with spin-wave calculations on the sublattice magnetization in single-layer structures,[12] it is not expected that further renormalization will improve matters. The breakdown therefore indicates that above this point a kind of excitations set in that are not properly accounted for by spin-wave theory. The present measurements, manifesting divergence of $\chi^{\parallel}$ near T_N, as well as analogous results for single-layer structures, indicate

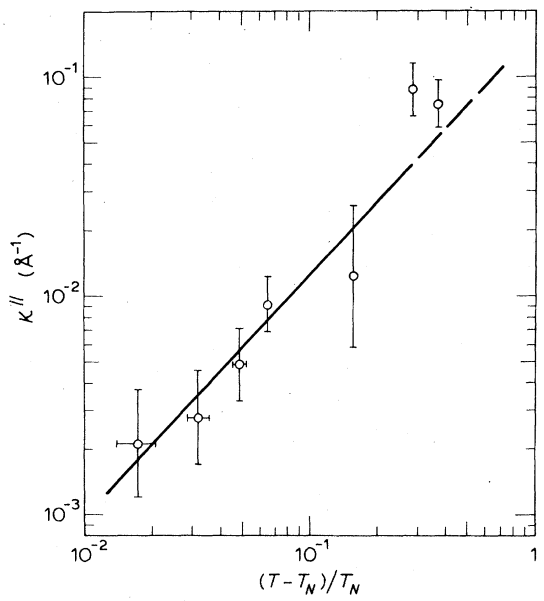

FIG. 8. Inverse correlation length $\kappa^{\parallel}$, as derived from the width of the scattering ridge at $(\frac{1}{2}\ \frac{1}{2}\ 1.46)$ vs the reduced temperature in a log-log plot. Similarly to Fig. 7, we have accounted for the transverse susceptibility and the spectrometer resolution.

that critical fluctuations involve longitudinal excitations rather than transverse ones.

(iii) In the critical regime, the order parameter follows a power law with a critical exponent $\beta = 0.154 \pm 0.006$, which essentially equals those found in single-layer Mn structures and approximates those in other 2-D systems.[9] In contrast, the coefficient $B = 0.83 \pm 0.03$, i.e., the power law extrapolated to zero temperature, differs from $B = 1.0 \pm 0.03$ in K_2MnF_4,[9] and even more from the 2-D Ising $B = 1.22$. One should however observe that B is not that directly connected with critical behavior. Rather, its value indicates how far the sublattice magnetization is already forced down by spin waves at the point where the critical regime is entered. In comparing $K_3Mn_2F_7$ and K_2MnF_4 (see Fig. 5) in the region where spin waves dominate, $1 > (T_N - T)/T_N > 0.3$ say, we see that the decrement of the reduced sublattice magnetization is larger in $K_3Mn_2F_7$, simply because at a certain T/T_N there is a larger number of spin waves excited. By similar arguments, the result from neutron data in K_2NiF_4 that a power law fitted to the sublattice magnetization holds from the critical regime all the way down to 4.2 K,[6] should be considered a matter of coincidence, and, in fact, is not borne out by the more accurate NMR results.[12]

(iv) The critical part of the scattering remains on ridges in reciprocal space when approaching the phase transition from above. This by itself indicates that

the spin correlations remain 2-D down to T_N. It was further found that the critical exponents for the longitudinal generalized susceptibility and inverse correlation length, $\gamma = 1.9 \pm 0.3$ and $\nu = 1.1 \pm 0.2$, respectively, as extracted from the temperature variation of the ridge scattering profile, do not significantly differ from those in single-layer structures.[9] The correction to the classical Ornstein-Zernike form, $\eta = 0.20 \pm 0.05$, is also appropriate to 2-D systems.[9] Thus, all evidence from both above and below T_N leads to the general conclusion that the phase transition in Heisenberg double layers with weak anisotropy is of strictly 2-D nature.

It is of interest to compare the reduction of the correlation length with temperature with that in comparable 2-D and 3-D systems. In the double-layer structure $K_3Mn_2F_7$ the spatial correlations between the spins extend to about 100 Å at 1.1 T_N [cf. Eq.(10)]. At 1.1 T_N the correlation length in $KMnF_3$ is 12 Å,[29] whereas in the single-layer structures K_2NiF_4 and K_2MnF_4 the correlation within the layer extends over distances of 110 and 80 Å, respectively. It has been found that the correlation length is slightly sensitive to the magnetic anisotropy,[9] so that the above values may not be entirely comparable. Nevertheless, the relative magnitudes of these correlation lengths supply an additional argument for the conclusion that in the regime just above the ordering point, up to say $1.2T_N$, the double layer behaves as a strictly 2-D system.

Another point, which does not require the lengthy chain of analyzing leading to the critical coefficients, but instead is directly verifiable from experiment by observing the development of the scattering ridge with temperature, is the temperature at which 2-D correlations cease to exist. In the representative 2-D system K_2NiF_4 spin correlations within the planes are found to persist up to at least $2T_N$,[6] at which point the correlation length is still 23 Å. In contrast, in $K_3Mn_2F_7$ the ridge of 2-D critical scattering has virtually disappeared at $\sim 1.5T_N$. These results lead one to the conjecture that in the region 1.5 T_N and above $K_3Mn_2F_7$ is in the course of going over to 3-D behavior. A point of note here is that extrapolation of the power law in $K_3Mn_2F_7$ from the region $T < 1.2\,T_N$ to 1.5 T_N would yield a correlation length of ~ 5 Å. This is of the order of the paired-layer distance, and therefore indicative of the onset of breakdown of correlations in the z direction. The conjecture is also qualitatively consistent with deductions from the magnetic susceptibility,[1,2] which give evidence for a behavior intermediate between 2-D and 3-D in this regime.

Finally, we briefly discuss the results in relation to the findings from high-temperature expansion of the susceptibility in n-layer Heisenberg ferromagnets.[17] In case of a double-layer ferromagnet, from these calculations 2-D critical behavior is expected below, say $1.2T_{SK}$, with T_{SK} denoting the Stanley-Kaplan temperature at which the susceptibility is found to diverge by extrapolating the expansion to low temperatures. T_{SK} usually agrees reasonably with the true transition point T_N. Although the high-temperature series was evaluated for ferromagnets, it is noteworthy that the extent of the critical region found in the double-layer antiferromagnet $K_3Mn_2F_7$ is consistent with these results.

ACKNOWLEDGMENT

The authors are grateful to J.A.J. Basten for kindly making available to them his computer program for deconvolution of critical scattering data.

[1]R. Navarro, J. J. Smit, L. J. de Jongh, W. J. Crama, and D. J. W. IJdo, Physica B (Utr.) 83, 97 (1976).
[2]A. F. M. Arts, C. M. J. van Uijen, J. A. van Luijk, H. W. de Wijn, and C. J. Beers, Solid State Commun. 21, 13 (1977).
[3]A. F. M. Arts and H. W. de Wijn, Phys. Rev. B 15, 4348 (1977).
[4]A. van der Pol, M. P. H. Thurlings, and H. W. de Wijn, J. Magn. Magn. Mat. 6, 122 (1977).
[5]E. Legrand and R. Plumier, Phys. Status Solidi 2, 317 (1962).
[6]R. J. Birgeneau, H. J. Guggenheim, and G. Shirane, Phys. Rev. Lett. 22, 720 (1969); Phys. Rev. B 1, 2211 (1970).
[7]R. J. Birgeneau, H. J. Guggenheim, and G. Shirane, Phys. Rev. B 8, 304 (1973).
[8]R. J. Birgeneau, J. Skalyo, Jr., and G. Shirane, Phys. Rev. B 3, 1736 (1971).
[9]R. J. Birgeneau, J. Als-Nielsen, and G. Shirane, Phys. Rev. B 16, 280 (1977).
[10]D. J. Breed, thesis (University of Amsterdam, 1969) (unpublished); Physica (Utr.) 37, 35 (1967).
[11]For a review, L. J. de Jongh and A. R. Miedema, Adv. Phys. 23, 1 (1974).
[12]H. W. de Wijn, L. R. Walker and R. E. Walstedt, Phys. Rev. B 8, 285 (1973).
[13]N. D. Mermin and A. Wagner, Phys. Rev. Lett. 17, 1133 (1966).
[14]M. E. Lines, Phys. Rev. 164, 736 (1967).
[15]L. Onsager, Phys. Rev. 65, 117 (1944); Nuovo Cimento Suppl. 6, 261 (1949).
[16]E. Gurewitz, J. Makovsky, and H. Shaked, Phys. Rev. B 14, 2071 (1976).
[17]D. S. Ritchie and M. E. Fisher, Phys. Rev. B 7, 480 (1973).
[18]W. Marshall and R. D. Lowde, Rep. Prog. Phys. 31, 705 (1968).
[19]R. E. Watson and A. J. Freeman, Acta Crystallogr. 14, 27 (1961).
[20]R. J. Birgeneau, J. Skalyo, and G. Shirane, J. Appl. Phys. 41, 1303 (1970).

[21]R. L. Stephenson and P. J. Wood, J. Phys. C 3, 90 (1970); J. C. Le Guillou and J. Zinn-Justin, Phys. Rev. Lett. 39, 95 (1977); G. A. Baker, Jr., B. G. Nickel, and D. I. Meiron, Phys. Rev. 17, 1365 (1978).
[22]P. Heller, Phys. Rev. 146, 403 (1966).
[23]A. Tucciarone, H. Y. Lau, L. M. Corliss, A. Delapalme, and J. M. Hastings, Phys. Rev. B 4, 3206 (1971).
[24]M. J. Cooper and R. Nathans, Acta Crystallogr. A 24, 619 (1968).
[25]M. E. Fisher and R. J. Burford, Phys. Rev. 156, 583 (1967).
[26]C. M. J. van Uijen, A. F. M. Arts, and H. W. de Wijn (unpublished).
[27]M. P. Schulhof, P. Heller, R. Nathans, and A. Linz, Phys. Rev. B 1, 2304 (1970).
[28]H. Y. Lau, L. M. Corliss, A. Delapalme, J. M. Hastings, R. Nathans, and A. Tucciarone, J. Appl. Phys. 41, 1384 (1970).
[29]M. J. Cooper and R. Nathans, J. Appl. Phys. 37, 1041 (1966).
[30]H. Ikeda and K. Hirakawa, J. Phys. Soc. Jpn. 33, 393 (1972).